

## Observation of a Near-Threshold Enhancement in the $p\bar{p}$ Mass Spectrum from Radiative $J/\psi \rightarrow \gamma p\bar{p}$ Decays

J. Z. Bai,<sup>1</sup> Y. Ban,<sup>9</sup> J. G. Bian,<sup>1</sup> X. Cai,<sup>1</sup> J. F. Chang,<sup>1</sup> H. F. Chen,<sup>16</sup> H. S. Chen,<sup>1</sup> J. Chen,<sup>3</sup> Jie Chen,<sup>8</sup> J. C. Chen,<sup>1</sup> Y. B. Chen,<sup>1</sup> S. P. Chi,<sup>1</sup> Y. P. Chu,<sup>1</sup> X. Z. Cui,<sup>1</sup> Y. M. Dai,<sup>7</sup> Y. S. Dai,<sup>19</sup> L. Y. Dong,<sup>1</sup> S. X. Du,<sup>18</sup> Z. Z. Du,<sup>1</sup> W. Dunwoodie,<sup>13</sup> J. Fang,<sup>1</sup> S. S. Fang,<sup>1</sup> C. D. Fu,<sup>1</sup> H. Y. Fu,<sup>1</sup> L. P. Fu,<sup>6</sup> C. S. Gao,<sup>1</sup> M. L. Gao,<sup>1</sup> Y. N. Gao,<sup>14</sup> M. Y. Gong,<sup>1</sup> W. X. Gong,<sup>1</sup> S. D. Gu,<sup>1</sup> Y. N. Guo,<sup>1</sup> Y. Q. Guo,<sup>1</sup> Z. J. Guo,<sup>2</sup> S. W. Han,<sup>1</sup> F. A. Harris,<sup>15</sup> J. He,<sup>1</sup> K. L. He,<sup>1</sup> M. He,<sup>10</sup> X. He,<sup>1</sup> Y. K. Heng,<sup>1</sup> T. Hong,<sup>1</sup> H. M. Hu,<sup>1</sup> T. Hu,<sup>1</sup> G. S. Huang,<sup>1</sup> L. Huang,<sup>6</sup> X. P. Huang,<sup>1</sup> J. M. Izen,<sup>17</sup> X. B. Ji,<sup>1</sup> C. H. Jiang,<sup>1</sup> X. S. Jiang,<sup>1</sup> D. P. Jin,<sup>1</sup> S. Jin,<sup>1</sup> Y. Jin,<sup>1</sup> B. D. Jones,<sup>17</sup> Z. J. Ke,<sup>1</sup> D. Kong,<sup>15</sup> Y. F. Lai,<sup>1</sup> F. Li,<sup>1</sup> G. Li,<sup>1</sup> H. H. Li,<sup>5</sup> J. Li,<sup>1</sup> J. C. Li,<sup>1</sup> K. Li,<sup>6</sup> Q. J. Li,<sup>1</sup> R. B. Li,<sup>1</sup> R. Y. Li,<sup>1</sup> W. Li,<sup>1</sup> W. G. Li,<sup>1</sup> X. Q. Li,<sup>8</sup> X. S. Li,<sup>14</sup> C. F. Liu,<sup>18</sup> C. X. Liu,<sup>1</sup> Fang Liu,<sup>16</sup> F. Liu,<sup>5</sup> H. M. Liu,<sup>1</sup> J. B. Liu,<sup>1</sup> J. P. Liu,<sup>18</sup> R. G. Liu,<sup>1</sup> Y. Liu,<sup>1</sup> Z. A. Liu,<sup>1</sup> Z. X. Liu,<sup>1</sup> X. C. Lou,<sup>17</sup> G. R. Lu,<sup>4</sup> F. Lu,<sup>1</sup> H. J. Lu,<sup>16</sup> J. G. Lu,<sup>1</sup> Z. J. Lu,<sup>1</sup> X. L. Luo,<sup>1</sup> E. C. Ma,<sup>1</sup> F. C. Ma,<sup>7</sup> J. M. Ma,<sup>1</sup> R. Malchow,<sup>3</sup> Z. P. Mao,<sup>1</sup> X. C. Meng,<sup>1</sup> X. H. Mo,<sup>2</sup> J. Nie,<sup>1</sup> Z. D. Nie,<sup>1</sup> S. L. Olsen,<sup>15</sup> D. Paluselli,<sup>15</sup> H. P. Peng,<sup>16</sup> N. D. Qi,<sup>1</sup> C. D. Qian,<sup>11</sup> J. F. Qiu,<sup>1</sup> G. Rong,<sup>1</sup> D. L. Shen,<sup>1</sup> H. Shen,<sup>1</sup> X. Y. Shen,<sup>1</sup> H. Y. Sheng,<sup>1</sup> F. Shi,<sup>1</sup> L. W. Song,<sup>1</sup> H. S. Sun,<sup>1</sup> S. S. Sun,<sup>16</sup> Y. Z. Sun,<sup>1</sup> Z. J. Sun,<sup>1</sup> S. Q. Tang,<sup>1</sup> X. Tang,<sup>1</sup> D. Tian,<sup>1</sup> Y. R. Tian,<sup>14</sup> W. Toki,<sup>3</sup> G. L. Tong,<sup>1</sup> G. S. Varner,<sup>15</sup> J. Wang,<sup>1</sup> J. Z. Wang,<sup>1</sup> L. Wang,<sup>1</sup> L. S. Wang,<sup>1</sup> M. Wang,<sup>1</sup> Meng Wang,<sup>1</sup> P. Wang,<sup>1</sup> P. L. Wang,<sup>1</sup> W. F. Wang,<sup>1</sup> Y. F. Wang,<sup>1</sup> Zhe Wang,<sup>1</sup> Z. Wang,<sup>1</sup> Zheng Wang,<sup>1</sup> Z. Y. Wang,<sup>2</sup> C. L. Wei,<sup>1</sup> N. Wu,<sup>1</sup> X. M. Xia,<sup>1</sup> X. X. Xie,<sup>1</sup> G. F. Xu,<sup>1</sup> Y. Xu,<sup>1</sup> S. T. Xue,<sup>1</sup> M. L. Yan,<sup>16</sup> W. B. Yan,<sup>1</sup> G. A. Yang,<sup>1</sup> H. X. Yang,<sup>14</sup> J. Yang,<sup>16</sup> S. D. Yang,<sup>1</sup> M. H. Ye,<sup>2</sup> Y. X. Ye,<sup>16</sup> J. Ying,<sup>9</sup> C. S. Yu,<sup>1</sup> G. W. Yu,<sup>1</sup> C. Z. Yuan,<sup>1</sup> J. M. Yuan,<sup>1</sup> Y. Yuan,<sup>1</sup> Q. Yue,<sup>1</sup> S. L. Zang,<sup>1</sup> Y. Zeng,<sup>6</sup> B. X. Zhang,<sup>1</sup> B. Y. Zhang,<sup>1</sup> C. C. Zhang,<sup>1</sup> D. H. Zhang,<sup>1</sup> H. Y. Zhang,<sup>1</sup> J. Zhang,<sup>1</sup> J. M. Zhang,<sup>4</sup> J. W. Zhang,<sup>1</sup> L. S. Zhang,<sup>1</sup> Q. J. Zhang,<sup>1</sup> S. Q. Zhang,<sup>1</sup> X. Y. Zhang,<sup>10</sup> Y. J. Zhang,<sup>9</sup> Yiyun Zhang,<sup>12</sup> Y. Y. Zhang,<sup>1</sup> Z. P. Zhang,<sup>16</sup> D. X. Zhao,<sup>1</sup> Jiawei Zhao,<sup>16</sup> J. W. Zhao,<sup>1</sup> P. P. Zhao,<sup>1</sup> W. R. Zhao,<sup>1</sup> Y. B. Zhao,<sup>1</sup> Z. G. Zhao,<sup>1,\*</sup> J. P. Zheng,<sup>1</sup> L. S. Zheng,<sup>1</sup> Z. P. Zheng,<sup>1</sup> X. C. Zhong,<sup>1</sup> B. Q. Zhou,<sup>1</sup> G. M. Zhou,<sup>1</sup> L. Zhou,<sup>1</sup> N. F. Zhou,<sup>1</sup> K. J. Zhu,<sup>1</sup> Q. M. Zhu,<sup>1</sup> Yingchun Zhu,<sup>1</sup> Y. C. Zhu,<sup>1</sup> Y. S. Zhu,<sup>1</sup> Z. A. Zhu,<sup>1</sup> B. A. Zhuang,<sup>1</sup> and B. S. Zou.<sup>1</sup>

(BES Collaboration)

<sup>1</sup>*Institute of High Energy Physics, Beijing 100039, People's Republic of China*

<sup>2</sup>*China Center of Advanced Science and Technology, Beijing 100080, People's Republic of China*

<sup>3</sup>*Colorado State University, Fort Collins, Colorado 80523, USA*

<sup>4</sup>*Henan Normal University, Xinxiang 453002, People's Republic of China*

<sup>5</sup>*Huazhong Normal University, Wuhan 430079, People's Republic of China*

<sup>6</sup>*Hunan University, Changsha 410082, People's Republic of China*

<sup>7</sup>*Liaoning University, Shenyang 110036, People's Republic of China*

<sup>8</sup>*Nankai University, Tianjin 300071, People's Republic of China*

<sup>9</sup>*Peking University, Beijing 100871, People's Republic of China*

<sup>10</sup>*Shandong University, Jinan 250100, People's Republic of China*

<sup>11</sup>*Shanghai Jiaotong University, Shanghai 200030, People's Republic of China*

<sup>12</sup>*Sichuan University, Chengdu 610064, People's Republic of China*

<sup>13</sup>*Stanford Linear Accelerator Center, Stanford, California 94309, USA*

<sup>14</sup>*Tsinghua University, Beijing 100084, People's Republic of China*

<sup>15</sup>*University of Hawaii, Honolulu, Hawaii 96822, USA*

<sup>16</sup>*University of Science and Technology of China, Hefei 230026, People's Republic of China*

<sup>17</sup>*University of Texas at Dallas, Richardson, Texas 75083-0688, USA*

<sup>18</sup>*Wuhan University, Wuhan 430072, People's Republic of China*

<sup>19</sup>*Zhejiang University, Hangzhou 310028, People's Republic of China*

(Received 7 March 2003; published 10 July 2003)

We observe a narrow enhancement near  $2m_p$  in the invariant mass spectrum of  $p\bar{p}$  pairs from radiative  $J/\psi \rightarrow \gamma p\bar{p}$  decays. No similar structure is seen in  $J/\psi \rightarrow \pi^0 p\bar{p}$  decays. The results are based on an analysis of a  $58 \times 10^6$  event sample of  $J/\psi$  decays accumulated with the BESII detector at the Beijing electron-positron collider. The enhancement can be fit with either an  $S$ - or  $P$ -wave Breit-Wigner resonance function. In the case of the  $S$ -wave fit, the peak mass is below  $2m_p$  at  $M = 1859^{+3}_{-10}$  (stat) $^{+5}_{-25}$  (syst) MeV/ $c^2$  and the total width is  $\Gamma < 30$  MeV/ $c^2$  at the 90% confidence level. These mass and width values are not consistent with the properties of any known particle.

There is an accumulation of evidence for anomalous behavior in the proton-antiproton ( $p\bar{p}$ ) system very near the  $M_{p\bar{p}} = 2m_p$  mass threshold. The observed cross section for  $e^+e^- \rightarrow$  hadrons has a narrow dipeake structure at a center of mass energy of  $\sqrt{s} \simeq 2m_p c^2$  [1]. The proton's timelike magnetic form factor, determined from high statistics measurements of the  $p\bar{p} \rightarrow e^+e^-$  annihilation process, exhibits a very steep falloff just above the  $p\bar{p}$  mass threshold [2]. The authors of Ref. [1] attribute these features to a narrow, subthreshold  $J^{PC} = 1^{--}$  resonance with mass  $1870 \pm 10$  MeV/ $c^2$  and width  $\Gamma = 10 \pm 5$  MeV/ $c^2$ . In studies of  $\bar{p}$  annihilations at rest in deuterium, anomalies in the charged pion momentum spectrum from  $\bar{p}d \rightarrow \pi^- \pi^0 p$  and  $\pi^+ \pi^- n$  reactions [3] and the proton spectrum from  $\bar{p}d \rightarrow p 2\pi^+ 3\pi^-$  [4] have been interpreted as effects of narrow, below-threshold resonances. There are no well established mesons that could be associated with such a state. The proximity in mass to  $2m_p$  is suggestive of nucleon-antinucleon ( $N\bar{N}$ ) bound states, an idea that has a long history. In 1949, Fermi and Yang [5] proposed that the pion was a tightly bound  $N\bar{N}$  state. Nambu and Jona-Lasinio [6] expanded on this in 1961 with a model based on chiral symmetry that has, in addition to a low-mass pion, a scalar  $p\bar{p}$  composite state with mass equal to  $2m_p$ . Although these ideas have been superseded by the quark model [7], the possibility of bound  $N\bar{N}$  states with mass near  $2m_p$ , generally referred to as *baryonium*, continues to be considered [8]. Recently Belle has reported observations of the decays  $B^+ \rightarrow K^+ p\bar{p}$  [9] and  $\bar{B}^0 \rightarrow D^0 p\bar{p}$  [10]. In both processes there are enhancements in the  $p\bar{p}$  invariant mass distributions near  $M_{p\bar{p}} \simeq 2m_p$ . An investigation of low-mass  $p\bar{p}$  systems with different quantum numbers may help clarify the situation.

In this Letter we report a study of the low-mass  $p\bar{p}$  pairs produced via radiative decays in a sample of  $58 \times 10^6$   $J/\psi$  events accumulated in the upgraded Beijing Spectrometer (BESII) located at the Beijing Electron-Positron Collider (BEPC) at the Beijing Institute of High Energy Physics. This reaction produces  $p\bar{p}$  systems with even  $C$  parity and, thus, probes states with different quantum numbers than those studied in Refs. [1,2].

BESII is a large solid-angle magnetic spectrometer that is described in detail in Ref. [11]. Charged particle momenta are determined with a resolution of  $\sigma_p/p = 1.78\% \sqrt{1 + p^2(\text{GeV}^2)}$  in a 40-layer cylindrical drift chamber. Particle identification is accomplished by specific ionization ( $dE/dx$ ) measurements in the drift chamber and time-of-flight (TOF) measurements in a barrel-like array of 48 scintillation counters. The  $dE/dx$  resolution is  $\sigma_{dE/dx} = 8.0\%$ ; the TOF resolution is  $\sigma_{\text{TOF}} = 180$  ps; both systems independently provide more than  $3\sigma$  separation of protons from any other charged particle species for the entire momentum range considered in this experiment. Radially outside of the time-of-flight counters is a 12-radiation-length barrel

shower counter (BSC) comprised of gas proportional tubes interleaved with lead sheets. The BSC measures the energies and directions of photons with resolutions of  $\sigma_E/E \simeq 21\%/\sqrt{E(\text{GeV})}$ ,  $\sigma_\phi = 7.9$  mrad, and  $\sigma_z = 2.3$  mrad. The iron flux return of the magnet is instrumented with three double layers of counters that are used to identify muons.

For this analysis we use events with a high energy gamma ray and two oppositely charged tracks each of which is well fitted to a helix originating near the interaction point. Candidate  $\gamma$ 's are associated with energy clusters in the BSC that have less than 80% of their total energy in any one readout layer and do not match the extrapolated position of any charged track. Since antiprotons that stop in the material of the TOF or BSC can produce annihilation products that are reconstructed elsewhere in the detector as  $\gamma$  rays, no restrictions are placed on the total number of neutral clusters in the event. We use charged tracks and  $\gamma$ 's that are within the polar angle region  $|\cos\theta| < 0.8$  and reject events where both tracks are identified as muons, or produce high energy showers in the BSC that are characteristic of electrons. The  $dE/dx$  information is used to form particle identification confidence levels  $\mathcal{P}_{\text{pid}}^i$ , where  $i$  denotes  $\pi$ ,  $K$ , and  $p$ . We require that both charged tracks have  $\mathcal{P}_{\text{pid}}^p > \mathcal{P}_{\text{pid}}^K$  and  $\mathcal{P}_{\text{pid}}^p > \mathcal{P}_{\text{pid}}^\pi$ . A study based on a kinematically selected sample of  $J/\psi \rightarrow K^{*\pm} K^\mp \rightarrow K^+ K^- \pi^0$  events indicates that the probability for a charged kaon to satisfy this requirement is less than 1% per track.

We subject the surviving events to four-constraint kinematic fits to the hypotheses  $J/\psi \rightarrow \gamma p\bar{p}$  and  $J/\psi \rightarrow \gamma K^+ K^-$ . For events with more than one  $\gamma$ , we select the  $\gamma$  that has the highest fit confidence level (C.L.). We select events that have fit confidence level  $\text{C.L.}_{\gamma p\bar{p}} > 0.05$  and reject events that have  $\text{C.L.}_{\gamma K^+ K^-} > \text{C.L.}_{\gamma p\bar{p}}$ .

Figure 1 shows the  $p\bar{p}$  invariant mass distribution for surviving events. The distribution has a peak near  $M_{p\bar{p}} = 2.98$  GeV/ $c^2$  that is consistent in mass, width, and yield with expectations for  $J/\psi \rightarrow \gamma \eta_c$ ,  $\eta_c \rightarrow p\bar{p}$  [12], a broad enhancement around  $M_{p\bar{p}} \sim 2.2$  GeV/ $c^2$ , and a narrow,

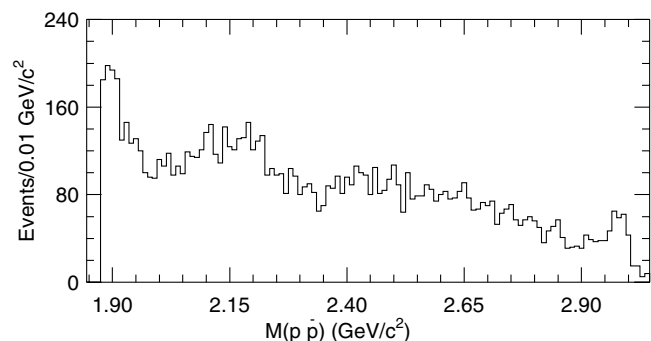


FIG. 1. The  $p\bar{p}$  invariant mass distribution for the  $J/\psi \rightarrow \gamma p\bar{p}$ -enriched event sample.

low-mass peak at the  $p\bar{p}$  mass threshold that is the subject of this Letter.

Backgrounds from processes involving charged particles that are not protons and antiprotons are negligibly small. In addition to being well separated from other charged particles by the  $dE/dx$  measurements and the kinematic fit, the protons and antiprotons from the low  $M_{p\bar{p}}$  region stop in the TOF counters and, thus, have very characteristic BSC responses: protons do not produce any matching signals in the BSC while secondary particles from antiproton annihilation usually produce large signals. This asymmetric behavior is quite distinct from that for  $K^+K^-$ ,  $\pi^+\pi^-$ , or  $e^+e^-$  pairs, where the positive and negative tracks produce similar, nonzero BSC responses. The observed BSC energy distributions for the selected  $J/\psi \rightarrow \gamma p\bar{p}$  events with  $M_{p\bar{p}} \leq 1.9 \text{ GeV}/c^2$  closely match expectations for protons and antiprotons and show no evidence for contamination from other particle species.

There is, however, a large background from  $J/\psi \rightarrow \pi^0 p\bar{p}$  events with an asymmetric  $\pi^0 \rightarrow \gamma\gamma$  decay where one of the photons has most of the  $\pi^0$ 's energy. This is studied using a sample of  $J/\psi \rightarrow \pi^0 p\bar{p}$  decays reconstructed from the same data sample. For these, we select events with oppositely charged tracks that are identified as protons and with two or more photons, apply a four-constraint kinematic fit to the hypothesis  $J/\psi \rightarrow \gamma\gamma p\bar{p}$ , and require  $\text{C.L.}_{\gamma\gamma p\bar{p}} > 0.005$ . For events with more than two  $\gamma$ 's, we select the  $\gamma$  pair that produces the best fit. In the  $M_{\gamma\gamma}$  distribution of the selected events there is a distinct  $\pi^0$  signal; we require  $|M_{\gamma\gamma} - M_{\pi^0}| < 0.03 \text{ GeV}/c^2$  ( $\pm 2\sigma$ ). The distribution of events vs  $M_{p\bar{p}} - 2m_p$  near the  $M_{p\bar{p}} = 2m_p$  threshold, shown in Fig. 2(a), is reasonably well described by a function of

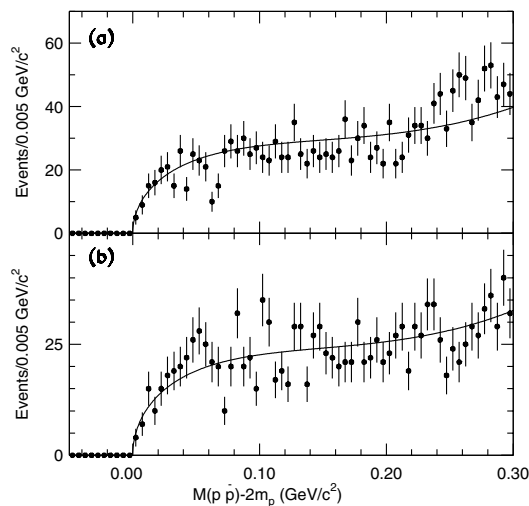


FIG. 2. The  $M_{p\bar{p}} - 2m_p$  distribution for (a) selected  $J/\psi \rightarrow \pi^0 p\bar{p}$  decays and (b) MC  $J/\psi \rightarrow \pi^0 p\bar{p}$  events that satisfy the  $\gamma p\bar{p}$  selection criteria. The smooth curves are the result of fits described in the text.

the form  $f_{\text{bkg}}(\delta) = N(\delta^{1/2} + a_1\delta^{3/2} + a_2\delta^{5/2})$ , where  $\delta \equiv M_{p\bar{p}} - 2m_p$  and the shape parameters  $a_1$  and  $a_2$  are determined from a fit to simulated Monte Carlo (MC) events that were generated uniformly in phase space. This is shown in the figure as a smooth curve. There is no indication of a narrow peak at low  $p\bar{p}$  invariant masses. Monte Carlo simulations of other  $J/\psi$  decay processes with final-state  $p\bar{p}$  pairs indicate that backgrounds from processes other than  $J/\psi \rightarrow \pi^0 p\bar{p}$  are negligibly small.

The  $M_{p\bar{p}} - 2m_p$  distribution for the  $\pi^0 p\bar{p}$  phase-space MC events that pass the  $\gamma p\bar{p}$  selection is shown in Fig. 2(b). There is no clustering at threshold; the smooth curve is the result of a fit to  $f_{\text{bkg}}(\delta)$  with the same shape parameter values.

In BESII, the detection efficiency for protons and antiprotons falls sharply for three momenta below  $0.4 \text{ GeV}/c$ . This produces a mass dependence in the experimental acceptance near  $M_{p\bar{p}} \simeq 2m_p$  for  $J/\psi \rightarrow \gamma p\bar{p}$  and  $\pi^0 p\bar{p}$ . For both processes, when  $M_{p\bar{p}}$  is very near  $2m_p$ , the  $p$  and  $\bar{p}$  both have three momenta very near  $0.5 \text{ GeV}/c$  and are well detected. For increasing  $p\bar{p}$  masses, more asymmetric energy sharing is possible and the acceptance decreases until  $M_{p\bar{p}} \simeq 2.0 \text{ GeV}/c^2$ , where it is  $\simeq 0.65$  of its value at  $M_{p\bar{p}} = 2m_p$ .

Figure 3(a) shows the threshold region for the selected  $J/\psi \rightarrow \gamma p\bar{p}$  events. The dotted curve in the figure indicates how the acceptance varies with invariant mass. The solid curve shows the result of a fit using an acceptance-weighted  $S$ -wave Breit-Wigner (BW) function [13] to represent the low-mass enhancement plus  $f_{\text{bkg}}(\delta)$  to

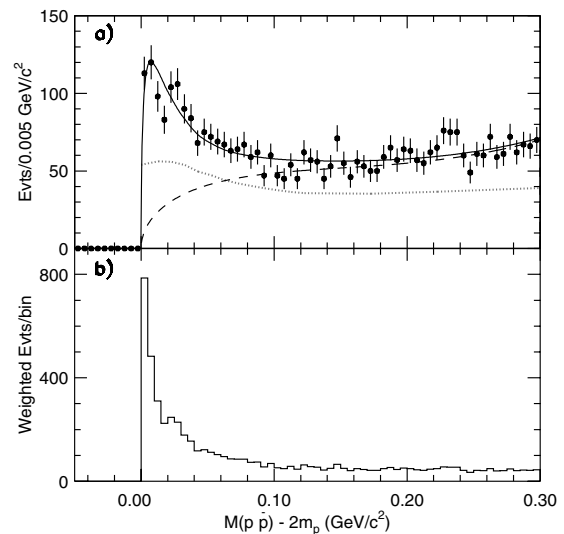


FIG. 3. (a) The near threshold  $M_{p\bar{p}} - 2m_p$  distribution for the  $\gamma p\bar{p}$  event sample. The solid curve is the result of the fit described in the text; the dashed curve shows the fitted background function. The dotted curve indicates how the acceptance varies with  $p\bar{p}$  invariant mass. (b) The  $M_{p\bar{p}} - 2m_p$  distribution with events weighted by  $q_0/q$ .

represent the background. The mass and width of the BW signal function are allowed to vary and the shape parameters of  $f_{\text{bkg}}(\delta)$  are fixed at the values derived from the fit to the  $\pi^0 p\bar{p}$  phase-space MC sample [14]. This fit yields  $928 \pm 57$  events [15] in the BW function with a peak mass of  $M = 1859^{+3}_{-10}$  MeV/ $c^2$  and a full width of  $\Gamma = 0 \pm 21$  MeV/ $c^2$ . Here the errors are statistical only: those for the event yield and the width are derived from the fit; the determination of the statistical errors for the mass is discussed below. The fit confidence level is 46.2% ( $\chi^2/\text{d.o.f.} = 56.3/56$ ).

Monte Carlo studies indicate that in the presence of background, the determination of the peak mass for a below-threshold resonance is more unreliable the further the peak position is below threshold. This produces an asymmetric distribution of mass input values that can produce our measured result. Moreover, the rms spread of these values increases for lower input masses, indicating that the statistical error returned by our mass fit underestimates the negative error. Because of this, we quote statistical errors for the mass that are derived from the rms spreads of fit results for an ensemble of MC experiments with different input mass values.

Further evidence that the peak mass is below the  $2m_p$  threshold is provided in Fig. 3(b), which shows the  $M_{p\bar{p}} - 2m_p$  distribution when the kinematic threshold behavior is removed by weighting each event by  $q_0/q$ , where  $q$  is the proton momentum in the  $p\bar{p}$  rest frame and  $q_0$  is the value for  $M_{p\bar{p}} = 2$  GeV/ $c^2$ . The sharp and monotonic increase at threshold that is observed in this weighted histogram can occur only for an  $S$ -wave BW function when the peak mass is below  $2m_p$ .

An  $S$ -wave  $p\bar{p}$  system with even  $C$  parity would correspond to a  $0^{-+}$  pseudoscalar state. We also tried to fit the signal with a  $P$ -wave BW function, which would correspond to a  $0^{++}$  ( ${}^3_0P$ ) scalar state that occurs in some models [6,8]. This fit yields a peak mass  $M = 1876.4 \pm 0.9$  MeV/ $c^2$ , which is very nearly equal to  $2m_p$ , and a very narrow total width:  $\Gamma = 4.6 \pm 1.8$  MeV/ $c^2$  (statistical errors only). The fit quality,  $\chi^2/\text{d.o.f.} = 59.0/56$ , is worse than that for the  $S$ -wave BW but still acceptable. A fit with a  $D$ -wave BW fails badly with  $\chi^2/\text{d.o.f.} = 1405/56$ .

In addition we tried fits that use known particle resonances to represent the low-mass peak. There are two spin-zero resonances listed in the Particle Data Group (PDG) tables in this mass region [16]: the  $\eta(1760)$  with  $M_{\eta(1760)} = 1760 \pm 11$  MeV/ $c^2$  and  $\Gamma_{\eta(1760)} = 60 \pm 16$  MeV/ $c^2$ , and the  $\pi(1800)$  with  $M_{\pi(1800)} = 1801 \pm 13$  MeV/ $c^2$  and  $\Gamma_{\pi(1800)} = 210 \pm 15$  MeV. A fit with  $f_{\text{bkg}}$  and an acceptance-weighted  $S$ -wave BW function with mass and width fixed at the PDG values for the  $\eta(1760)$  produces  $\chi^2/\text{d.o.f.} = 323.4/58$ . A fit using a BW with the  $\pi(1800)$  parameters is worse.

For both the scalar and pseudoscalar case, the polar angle of the photon,  $\theta_\gamma$ , would be distributed according

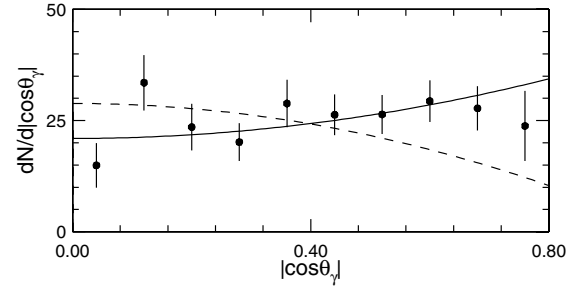


FIG. 4. The background-subtracted, acceptance-corrected  $|\cos\theta_\gamma|$  distribution for  $J/\psi \rightarrow \gamma p\bar{p}$ -enriched events with  $M_{p\bar{p}} \leq 1.9$  GeV/ $c^2$ . The solid curve is a fit to a  $1 + \cos^2\theta_\gamma$  shape for the region  $|\cos\theta_\gamma| \leq 0.8$ ; the dashed curve is the result of a fit to  $\sin^2\theta_\gamma$ .

to  $1 + \cos^2\theta_\gamma$ . Figure 4 shows the background-subtracted, acceptance-corrected  $|\cos\theta_\gamma|$  distribution for events with  $M_{p\bar{p}} \leq 1.9$  GeV and  $|\cos\theta_\gamma| \leq 0.8$ . Here we have subtracted the  $|\cos\theta_{\pi^0}|$  distribution from the  $\pi^0 p\bar{p}$  data sample, normalized to the area of  $f_{\text{bkg}}(\delta)$  for  $M_{p\bar{p}} < 1.9$  GeV/ $c^2$  to account for background. The solid curve shows the result of a fit for  $1 + \cos^2\theta_\gamma$  to the  $|\cos\theta_\gamma| < 0.8$  region; the dashed line shows the result of a similar fit to  $\sin^2\theta_\gamma$ . Although the data are not precise enough to establish a  $1 + \cos^2\theta_\gamma$  behavior, the distribution is consistent with expectations for a radiative transition to a pseudoscalar or scalar meson [17].

We evaluate systematic errors on the mass and width from changes observed in the fitted values for fits with different bin sizes, with background shape parameters left as free parameters, different shapes for the acceptance variation, and different resolutions. The ensemble Monte Carlo studies mentioned above indicate that in the presence of background, the determination of the parameters of a subthreshold BW resonance can be biased. We include the range of differences between input and output values seen in the MC study in the systematic errors.

For the mass, we determine a systematic error of  ${}^{+5}_{-25}$  MeV/ $c^2$ . For the total width, we determine a 90% confidence level upper limit of  $\Gamma < 30$  MeV/ $c^2$ , where the limit includes the systematic error.

Using a Monte Carlo determined acceptance of 23%, we determine a product of branching fractions  $\mathcal{B}(J/\psi \rightarrow \gamma X)\mathcal{B}(X \rightarrow p\bar{p}) = 7.0 \pm 0.4(\text{stat})^{+1.9}_{-0.8}(\text{syst}) \times 10^{-5}$ , where the systematic error includes uncertainties in the acceptance (10%), the total number of  $J/\psi$  decays in the data sample (5%), and the effects of changing the various inputs to the fit ( ${}^{+24\%}_{-2\%}$ ).

In summary, we observe a strong, near-threshold enhancement in the  $p\bar{p}$  invariant mass distribution in the radiative decay process  $J/\psi \rightarrow \gamma p\bar{p}$ . No similar structure is seen in  $J/\psi \rightarrow \pi^0 p\bar{p}$  decays. The structure has properties consistent with either a  $J^{PC} = 0^{-+}$  or  $0^{++}$  quantum number assignment and cannot be attributed to the effects of any known meson resonance. If interpreted as a single

$0^{-+}$  resonance, its peak mass is below the  $M_{p\bar{p}} = 2m_p$  threshold at  $1859_{-10}^{+3}(\text{stat})_{-25}^{+5}(\text{syst})$  MeV/ $c^2$  and its width is  $\Gamma < 30$  MeV/ $c^2$  at the 90% C.L. These mass and width values are close to those of the  $1^{--}$  state discussed in Ref. [1], which suggests that these states may be related. A search for a state with these properties in radiative  $J/\psi$  decays to mesonic final states is in progress.

We thank the staffs of BEPC and the computing center for their strong efforts. This work is supported in part by the National Natural Science Foundation of China under Contracts No. 19991480, No. 10225524, and No. 10225525 and the Chinese Academy of Sciences under Contract No. KJ 95T-03, the 100 Talents Program of CAS under Contracts No. U-24 and No. U-25, and the Knowledge Innovation Project of CAS under Contracts No. U-602 and No. U-34 (IHEP); by the National Natural Science Foundation of China under Contract No. 10175060 (USTC); and by the Department of Energy under Contracts No. DE-FG03-93ER40788 (Colorado State University), No. DE-AC03-76SF00515 (SLAC), No. DE-FG03-94ER40833 (U. Hawaii), and No. DE-FG03-95ER40925 (UT Dallas).

---

\*Visiting scientist at the University of Michigan, Ann Arbor, MI 48109, USA.

- [1] FENICE Collaboration, A. Antonelli *et al.*, Nucl. Phys. **B517**, 3 (1998).
- [2] G. Bardin *et al.*, Nucl. Phys. **B411**, 3 (1994).
- [3] D. Bridges *et al.*, Phys. Lett. B **180**, 313 (1986).
- [4] O. D. Dalkarov *et al.*, Phys. Lett. B **392**, 229 (1997).
- [5] E. Fermi and C. N. Yang, Phys. Rev. **76**, 1739 (1949).
- [6] Y. Nambu and G. Jona-Lasinio, Phys. Rev. **122**, 345 (1961); **124**, 246 (1961).
- [7] R. Delbourgo and M. D. Scadron, Phys. Rev. Lett. **48**, 379 (1982); T. Hatsuda and T. Kunihiro, Prog. Theor. Phys. **74**, 765 (1985); Phys. Rep. **247**, 221 (1994).
- [8] For recent reviews of this subject, see E. Klempt *et al.*, Phys. Rep. **368**, 119 (2002); J.-M. Richard, Nucl. Phys. B (Proc. Suppl.) **86**, 361 (2000).
- [9] Belle Collaboration, K. Abe *et al.*, Phys. Rev. Lett. **88**, 181803 (2002).
- [10] Belle Collaboration, K. Abe *et al.*, Phys. Rev. Lett. **89**, 151802 (2002).
- [11] BES Collaboration, J. Z. Bai *et al.*, Nucl. Instrum. Methods Phys. Res., Sect. A **458**, 627 (2001).
- [12] BES Collaboration, J. Z. Bai *et al.*, Phys. Lett. B **555**, 174 (2003).
- [13] For the BW, we use the form  $\text{BW}(M) \propto \frac{q^{(2\ell+1)}k^3}{(M^2 - M_0^2)^2 + M_0^2\Gamma^2}$ , where  $\Gamma$  is a constant (determined from the fit),  $q$  is the proton momentum in the  $p\bar{p}$  rest frame,  $\ell$  is the  $p\bar{p}$  orbital angular momentum, and  $k$  is the photon momentum. Note that for  $M_0 < 2m_p$ , the BW tail above  $M_{p\bar{p}} = 2m_p$  is substantial, even for  $\Gamma = 0$ .
- [14] The  $p\bar{p}$  mass resolution varies from  $\sigma \simeq 1.2$  MeV/ $c^2$  at  $M_{p\bar{p}} \simeq 2m_p$  to  $\sim 3$  MeV/ $c^2$  at higher masses. Convoluting the fitting function with a Gaussian with a width in this range has no significant effect on the results.
- [15] The background level in the fit is about twice the level of  $J/\psi \rightarrow \pi^0 p\bar{p}$  feedthrough predicted by the MC. This indicates that there is some contribution from nonresonant three-body  $J/\psi \rightarrow \gamma p\bar{p}$  decays.
- [16] Particle Data Group, D. Groom *et al.*, Eur. Phys. J. C **15**, 1 (2000).
- [17] The  $1 + \cos^2\theta_\gamma$  fit has  $\chi^2/\text{d.o.f.} = 3.7/7$ ; the  $\sin^2\theta_\gamma$  fit has  $\chi^2/\text{d.o.f.} = 10.3/7$ .